

# Image Registration via Particle Movement

Zhao Yi and Justin Wan

## Abstract

Though fluid model offers a good approach to nonrigid registration with large deformations, it suffers from the blurring artifacts introduced by the viscosity term. To overcome this drawback, we present an inviscid model expressed in a particle framework. Our idea is to simulate the template image as a set of particles moving towards the target positions. The proposed model can accommodate both small and large deformations with sharp edges and reasonable displacement maps achieved. Because of its simplicity, the computational cost is much smaller than other nonrigid registration approaches.

## 1 INTRODUCTION

Image registration requires aligning an image pair with an optimal transformation. It has many potential applications for diagnosing in the clinic, and is an often encountered problem in various fields especially in medical surgery.

It is well known that biological structures such as human brains, although may contain the same global structures, differ in shape, orientation, and fine structures across individuals and at different times. To represent such variabilities, nonrigid transformation has more applications [10]. Numerous algorithms have been explored in this area, however, more accurate and efficient methods are still needed. Broit [3] was the first to study nonrigid registration problems using physically based models. In his approach the transformation process was modeled by deformations of an elastic solid. This approach was extended by Bajcsy et al. [1] and various variational forms [4, 8] were proposed later. Since the deformation energy caused by stress increases proportionally with the strength of the deformation, elastic models can only accommodate locally small deformations. To overcome this drawback, Christensen et al. [6] proposed another approach which modeled the transformation process by a viscous fluid flow. Fluid models can allow relatively larger local deformations; however, the inherent viscosity introduces an unnegligible blurring effect to the transformed image. Also, the reported [2, 12] computational time is very large. The models discussed above are all physically based models, which try to simulate the deformation as a physical process.

Since the viscosity term in the fluid equation causes blurring as well as complicating computation, we propose to use an inviscid model. Instead of regarding the template image as a fluid continuum with viscous interaction, we

simulate the transformation process as a set of particles moving towards target positions. It is similar to the framework of gas dynamics [9] where distances between gas molecules are big enough that internal friction can be neglected and each molecule can be viewed as a separate particle.

Particles are by far the easiest objects to simulate. Despite their simplicity, particles can be made to exhibit a wide range of interesting behaviors. For example, in graphics [7] a variety of nonrigid structures can be built by connecting particles with simple damped springs. However, the particle approach has never been used in image registration area. Based on the physical behavior of particles, we present a novel registration technique expressed in a particle framework. The basic idea is to simulate the template image as particles moving towards the target image under external forces. Lagrangian reference frame is often used to observe the movement of particles. However, it needs to track individual particle and is harder to apply. As time varies, initially equally-sized particles may become unevenly distributed which can cause problems of stability and accuracy. Assuming there are enough particles moving around, we can fit Eulerian reference frame to the particle registration framework. The resulting partial differential equations are nonlinear hyperbolic equations of vector form whose solution describes the coordinate transformation between the template and the target images. They can be numerically solved using finite difference method.

The proposed particle registration technique is quite simple and efficient. Since it can be viewed as an inviscid gas model with constant pressure, the blurring artifacts caused by fluid viscosity are overcome and large deformation can be accommodated. Also, because of its simplicity in simulation, total computational cost is decreased. Thus, the particle registration technique can achieve a small/large transformed image with sharp edges and reasonable displacement map in less time. We have successfully applied the particle model to medical image datasets yielding fast and accurate registrations.

A relevant approach was the level-set registration technique proposed by Vemuri et al. [11]. As an inviscid model, their approach was derived from curve evolution theory which had different settings and governing equations, and thus could not be regarded as a particle framework.

The rest of the paper is organized as follows. Section 2 contains an overview of the particle model, followed by the proposed formulation of the image registration problem. Section 3 presents some modifications of the model regarding robustness and stability, and gives the whole numerical algorithm for solving the consequent equations. Section 4 shows experimental results of this approach on 2D sythetic/real images. Finally, conclusions are drawn in Section 5.

## 2 METHODOLOGY

We define the template image as  $I_1(\mathbf{x})$  and the target image as  $I_2(\mathbf{x})$ , where  $0 \leq I_1(\mathbf{x}), I_2(\mathbf{x}) \leq 1$ , and  $\mathbf{x} \in \Omega$  is the image region. The purpose of image registration is to determine a coordinate transformation  $\mathbf{r}(\mathbf{x})$  of  $I_1(\mathbf{x})$  onto  $I_2(\mathbf{x})$

such that the difference between the transformed template image  $I_1(\mathbf{x} - \mathbf{r}(\mathbf{x}))$  and the target image  $I_2(\mathbf{x})$  will be small in some measure  $M$ . Therefore the registration can also be stated as a minimization problem

$$\min_{\mathbf{r}(\mathbf{x})} M(I_1(\mathbf{x}), I_2(\mathbf{x}), \mathbf{r}(\mathbf{x})). \quad (1)$$

Here we use a Gaussian sensor model [5] to induce the matching criteria:

$$M(I_1(\mathbf{x}), I_2(\mathbf{x}), \mathbf{r}(\mathbf{x}, t)) = \frac{\alpha'}{2} \int_{\Omega} \|I_1(\mathbf{x} - \mathbf{r}(\mathbf{x}, t)) - I_2(\mathbf{x})\|^2 d\mathbf{x}, \quad (2)$$

where  $\alpha'$  is a parameter.

We consider the template image as a set of particles, each with mass  $m$ , position  $\mathbf{x}$ , velocity  $\mathbf{u}$ , displacement  $\mathbf{r}$ , and responding to force. The image deformation process is simulated as the particles moving towards the target positions. The total number of particles is assumed to be big enough such that at anytime there is a particle passing through each observation point. Thus, we can use Eulerian reference frame for simulation. The image region  $\Omega$  is discretized into a fixed grid and motion of particles is controlled in each cell. The velocity field  $\mathbf{u}(\mathbf{x})$  and the displacement field  $\mathbf{r}(\mathbf{x})$  are both defined based on current positions of particles. A particle at position  $\mathbf{x}$  at time  $t$  originated at position  $\mathbf{x} - \mathbf{r}(\mathbf{x}, t)$ .

The movement of a particle is governed by Newton's Law of Motion. If we assume that there is no internal interaction between particles, the conservation of momentum equation can be written as

$$m \frac{d\mathbf{u}}{dt} = \mathbf{f}, \quad (3)$$

where  $\mathbf{f}$  is the external force applied to that particle and will be defined later by information from the template and the target images,  $m$  is the mass of each particle which is assumed to be a constant here,  $\mathbf{u}$  is the consequent velocity which describes the speed of image deformation, and  $t$  is the time.

In an Eulerian framework, we have the following relationship between total derivative and partial derivative of velocity with respect to time

$$\frac{d\mathbf{u}}{dt} = \frac{\partial \mathbf{u}}{\partial t} + (\mathbf{u} \cdot \nabla) \mathbf{u}, \quad (4)$$

where  $\nabla$  is the gradient operator. Thus, equation (3) can be rewritten as

$$m \frac{\partial \mathbf{u}}{\partial t} + m(\mathbf{u} \cdot \nabla) \mathbf{u} = \mathbf{f}. \quad (5)$$

The left side represents the force of inertia, i.e., the mass times the acceleration of a particle. Equation (5) neglects internal friction and therefore is an inviscid model. It is similar to the Euler equation commonly used in gas dynamics (the study of compressible but inviscid fluids)

$$\rho \frac{\partial \mathbf{u}}{\partial t} + \rho(\mathbf{u} \cdot \nabla) \mathbf{u} + \nabla p = \mathbf{f}, \quad (6)$$

where  $\rho$  is the density or unit mass, and  $p$  is the pressure. For isothermal gas with constant density,  $\nabla p$  is neglected and equation (6) becomes equation (5).

Since velocity is the total derivative of displacement with respect to time, the velocity field and the displacement field are related by

$$\mathbf{u}(\mathbf{x}, t) = \frac{d\mathbf{r}(\mathbf{x}, t)}{dt} = \frac{\partial \mathbf{r}(\mathbf{x}, t)}{\partial t} + \nabla \mathbf{r}(\mathbf{x}, t) \mathbf{u}(\mathbf{x}, t). \quad (7)$$

The force field  $\mathbf{f}(\mathbf{x}, \mathbf{r}(\mathbf{x}))$  is used to drive the particles from image  $I_1(\mathbf{x})$  to image  $I_2(\mathbf{x})$ . It is defined as the derivative of the matching criteria  $M$  on the image pair. Taking the variation of equation (2) with respect to displacement,  $\mathbf{r}(\mathbf{x}, t)$ , gives the force field

$$\mathbf{f}(\mathbf{x}, \mathbf{r}(\mathbf{x}, t)) = \alpha' (I_1(\mathbf{x} - \mathbf{r}(\mathbf{x}, t)) - I_2(\mathbf{x})) \nabla I_1(\mathbf{x} - \mathbf{r}(\mathbf{x}, t)). \quad (8)$$

Since the movement of particles should only slow down when the difference term  $I_1(\mathbf{x} - \mathbf{r}(\mathbf{x}, t)) - I_2(\mathbf{x})$  becomes smaller, we need to normalize the gradient term in the force field. Therefore we choose  $\alpha = \frac{\alpha'}{\|\nabla I_1\|}$  such that equation (8) becomes

$$\mathbf{f}(\mathbf{x}, \mathbf{r}(\mathbf{x}, t)) = \alpha (I_1(\mathbf{x} - \mathbf{r}(\mathbf{x}, t)) - I_2(\mathbf{x})) \frac{\nabla I_1(\mathbf{x} - \mathbf{r}(\mathbf{x}, t))}{\|\nabla I_1(\mathbf{x} - \mathbf{r}(\mathbf{x}, t))\|}. \quad (9)$$

### 3 IMPLEMENTATION

Solution of the particle registration problem requires solving the following PDEs

$$\begin{aligned} \frac{\partial \mathbf{u}(\mathbf{x}, t)}{\partial t} &= \frac{\mathbf{f}(\mathbf{x}, \mathbf{r}(\mathbf{x}, t))}{m} - (\mathbf{u} \cdot \nabla) \mathbf{u}(\mathbf{x}, t), \\ \frac{\partial \mathbf{r}(\mathbf{x}, t)}{\partial t} &= \mathbf{u}(\mathbf{x}, t) - \nabla \mathbf{r}(\mathbf{x}, t) \mathbf{u}(\mathbf{x}, t), \\ \mathbf{f}(\mathbf{x}, t) &= \alpha (I_1(\mathbf{x} - \mathbf{r}(\mathbf{x}, t)) - I_2(\mathbf{x})) \frac{\nabla I_1(\mathbf{x} - \mathbf{r}(\mathbf{x}, t))}{\|\nabla I_1(\mathbf{x} - \mathbf{r}(\mathbf{x}, t))\|}, \end{aligned}$$

which include nonlinearity introduced by the external force and the kinematic derivatives.

Two issues arise in calculating the external force field. The first is the undetermination of external force when  $\|\nabla I_1(\mathbf{x} - \mathbf{r}(\mathbf{x}, t))\|$  equals to zero. To make our model more robust, we apply an additive external force definition in that case:

$$\mathbf{f}(\mathbf{x}, \mathbf{r}(\mathbf{x}, t)) = 0. \quad (10)$$

The second is the computation of gradient  $\nabla I_1(\mathbf{x} - \mathbf{r}(\mathbf{x}, t))$ . Since the gradient operator is sensitive to the noise in the image, we convolve  $I_1(\mathbf{x} - \mathbf{r}(\mathbf{x}, t))$  with a Gaussian kernel prior to the gradient computation. Thus (9) and (10) become

$$\mathbf{f}(\mathbf{x}, \mathbf{r}(\mathbf{x}, t)) = \begin{cases} 0, & \text{if } \|\nabla(G_\sigma * I(\mathbf{x}, t))\| = 0; \\ \alpha (I(\mathbf{x}, t) - I_2(\mathbf{x})) \frac{\nabla(G_\sigma * I(\mathbf{x}, t))}{\|\nabla(G_\sigma * I(\mathbf{x}, t))\|}, & \text{otherwise;} \end{cases} \quad (11)$$

where  $I(\mathbf{x}, t) = I_1(\mathbf{x} - \mathbf{r}(\mathbf{x}, t))$  denotes the deformed template image at time  $t$ ,  $G_\sigma$  denotes the Gaussian kernel with standard deviation of  $\sigma$ , and  $*$  is the convolution operator.

To update movement of particles through time, we discretize time domain  $[0, +\infty]$  into small intervals  $0 = t_0 < t_1 < \dots < t_n < t_{n+1} < \dots$  and apply Euler explicit integration over time. The discretized time formula is given by

$$\begin{aligned}\mathbf{u}^{n+1}(\mathbf{x}) &= \mathbf{u}^n(\mathbf{x}) + \frac{\Delta t}{m} \mathbf{f}^n(\mathbf{x}), \\ \mathbf{r}^{n+1}(\mathbf{x}) &= \mathbf{r}^n(\mathbf{x}) + \Delta t (\mathcal{I} - \nabla \mathbf{r}^n(\mathbf{x})) \mathbf{u}^n(\mathbf{x}),\end{aligned}\quad (12)$$

where

$\mathbf{u}^{n+1}(\mathbf{x}) \approx \mathbf{u}(\mathbf{x}, t_{n+1})$  is the approximation of velocity field at time  $t_{n+1}$ ,  
 $\mathbf{r}^{n+1}(\mathbf{x}) \approx \mathbf{r}(\mathbf{x}, t_{n+1})$  is the approximation of displacement field at time  $t_{n+1}$ ,  
 $\Delta t = t_{n+1} - t_n$  is the time interval.

We require the Jacobian  $J = \|\mathcal{I} - \nabla \mathbf{r}^n\|$  [6] greater than zero in order to obtain a regular transformation. The complete algorithm for solving the particle registration problem consequently becomes

1. Initialize  $\mathbf{u}^0(\mathbf{x}) = \mathbf{0}$  and  $\mathbf{r}^0(\mathbf{x}) = \mathbf{0}$ .
2. Calculate the external force  $\mathbf{f}^n(\mathbf{x})$  at time  $t_n$  using equation (11).
3. If  $\mathbf{f}^n(\mathbf{x})$  is below a stopping criteria for all  $\mathbf{x}$  or the maximum number of iterations is reached, STOP.
4. Perform Euler explicit integration using equation (12) at time  $t_n$ .
5. If the Jacobian  $J = \|\mathcal{I} - \nabla \mathbf{r}^n(\mathbf{x})\|$  is less than 0.1, regrid the template.
6.  $n = n + 1$ , GOTO step 2.

The remaining question is how to perform steps 2, 4, and 5 in discretized space domain. Note that they all have gradient computation included. We choose minmod finite difference scheme since it is known to preserve local max/min and yield acceptable accuracy. The minmod function [11] is defined as

$$\text{minmod}(x, y) = \begin{cases} \text{sign}(x) \min(|x|, |y|), & \text{if } xy > 0; \\ 0, & \text{if } xy \leq 0; \end{cases}\quad (13)$$

and consequently the gradient is computed by

$$\nabla F(x, y) = \begin{bmatrix} \text{minmod}(D_x^- F, D_x^+ F) \\ \text{minmod}(D_y^- F, D_y^+ F) \end{bmatrix},\quad (14)$$

where  $F(x, y)$  is any 2D function,  $D_x^+$ ,  $D_x^-$ , and  $D_y^+$ ,  $D_y^-$  are standard forward and backward difference operators in the  $x$  and  $y$  directions, respectively.

To update movement of particles through space, we discretize space domain  $\Omega$  into small cells/pixels. Each particle is initially located at the center of the cell/pixel with position  $\mathbf{x}_{ij} = (x_i, y_j)$  and grid spacing  $h$ . Applying minmod finite difference over space, we obtain the discretized time discretized space formula

$$\begin{aligned}
f_{ij}^n &= \alpha(I_{ij}^n - I_{2,ij}) \frac{\minmod(\frac{I_{ij}^n - I_{i-1,j}^n}{h}, \frac{I_{i+1,j}^n - I_{ij}^n}{h})}{\|\minmod(\frac{I_{ij}^n - I_{i-1,j}^n}{h}, \frac{I_{i+1,j}^n - I_{ij}^n}{h})\|}, \\
g_{ij}^n &= \alpha(I_{ij}^n - I_{2,ij}) \frac{\minmod(\frac{I_{ij}^n - I_{i,j-1}^n}{h}, \frac{I_{i,j+1}^n - I_{ij}^n}{h})}{\|\minmod(\frac{I_{ij}^n - I_{i,j-1}^n}{h}, \frac{I_{i,j+1}^n - I_{ij}^n}{h})\|}, \\
u_{ij}^{n+1} &= u_{ij}^n + \Delta t f_{ij}^n, \\
v_{ij}^{n+1} &= v_{ij}^n + \Delta t g_{ij}^n, \\
r_{ij}^{n+1} &= r_{ij}^n + \Delta t((1 - \minmod(\frac{r_{ij}^n - r_{i-1,j}^n}{h}, \frac{r_{i+1,j}^n - r_{ij}^n}{h}))u_{ij}^n - \minmod(\frac{r_{ij}^n - r_{i,j-1}^n}{h}, \frac{r_{i,j+1}^n - r_{ij}^n}{h})v_{ij}^n), \\
s_{ij}^{n+1} &= s_{ij}^n + \Delta t((1 - \minmod(\frac{s_{ij}^n - s_{i,j-1}^n}{h}, \frac{s_{i,j+1}^n - s_{ij}^n}{h}))v_{ij}^n - \minmod(\frac{s_{ij}^n - s_{i-1,j}^n}{h}, \frac{s_{i+1,j}^n - s_{ij}^n}{h})u_{ij}^n),
\end{aligned}$$

where

$$\begin{aligned}
(f_{ij}^n, g_{ij}^n) &\approx \mathbf{f}(\mathbf{x}_{ij}, \mathbf{r}(\mathbf{x}_{ij}, t_n)) \text{ is the approximation of force at position } \mathbf{x}_{ij} \text{ time } t_n, \\
(u_{ij}^{n+1}, v_{ij}^{n+1}) &\approx \mathbf{u}(\mathbf{x}_{ij}, t_{n+1}) \text{ is the approximation of velocity at position } \mathbf{x}_{ij} \text{ time } t_{n+1}, \\
(r_{ij}^{n+1}, s_{ij}^{n+1}) &\approx \mathbf{r}(\mathbf{x}_{ij}, t_{n+1}) \text{ is the approximation of displacement at position } \mathbf{x}_{ij} \text{ time } t_{n+1}, \\
\Delta t &= t_{n+1} - t_n \text{ is the time interval,} \\
I_{ij}^n &= G_\sigma * I_{1,x_i - r_{ij}^n, y_j - s_{ij}^n} \text{ is the smoothed deformed template.}
\end{aligned}$$

The discretization is easily extendable to 3D.

## 4 RESULTS

The proposed approach is implemented in C and executed at a desktop PC of P4 2.8GHZ with 1GB memory. The parameters are set to  $m = 1$ ,  $\alpha = 100$ , and the stopping criteria is set to 0.01. We have applied the proposed algorithm to three experiments. Four sets of images are presented for each registration: 1. template image; 2. target image; 3. transformed image after registration; 4. difference image between transformed image and target image. The computational cost for each experiment is summarized in Table 1.

The first experiment is designed to demonstrate that our model can accommodate large deformation like fluid algorithm as well as achieving a reasonable displacement map. The test data is a synthetic image with size  $64 \times 64$  pixels which is similar to the image used by [6]. The results are shown in Figure 1 with comparison to fluid model. It is what we desire that the transformed image

Time(s)	experiment 1	experiment 2	experiment 3
Fluid	43	927	892
Proposed	32	644	532

Table 1: computational cost for each experiment

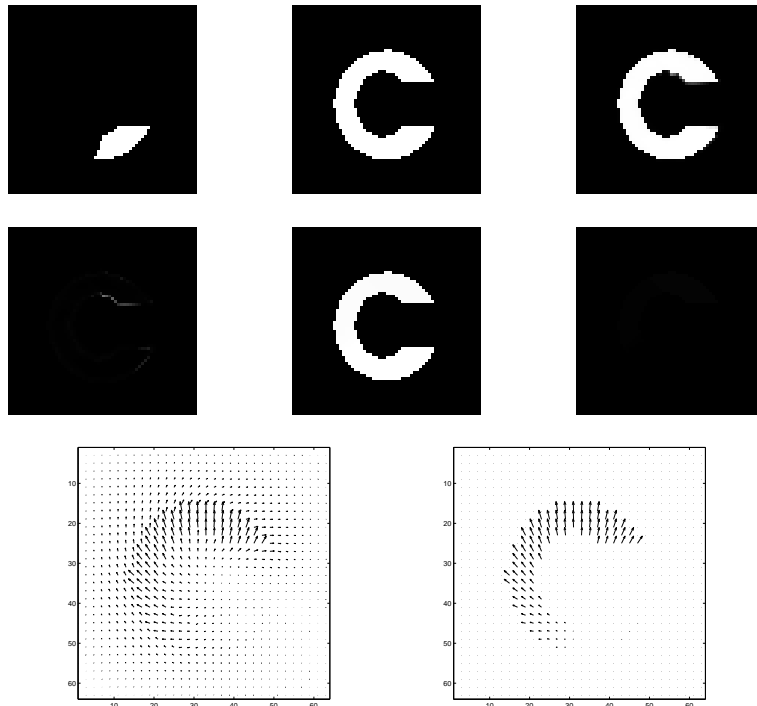


Figure 1: qualitative results of experiment 1. From left to right, top to bottom: (a)template image; (b)target image; (c)transformed image obtained by fluid model; (d)difference image between (b) and (c); (e)transformed image obtained by proposed model; (f)difference image between (b) and (f); (g)displacement map obtained by fluid model; (h)displacement map obtained by proposed model.

obtain by proposed model is almost the same as the target, and the difference image is better than that obtained by fluid model. Besides the four sets of images mentioned above, we include displacement map as well. For proposed model, it is largely curved from a small patch of letter "C" to the whole letter "C", and anywhere else is zero. This contrasts with the displacement map obtained by fluid model where background field also has nonzero displacements.

The second experiment is designed to demonstrate that our model can overcome the blurring drawback of fluid approach. The test data is a synthetic image with size  $256 \times 256$  pixels which is similar to the image used by [12]. The results are shown in Figure 2 with comparison to fluid model. Again we include displacement map in addition to the four sets of images mentioned above. From comparison we can see clearly that the difference image obtained by fluid model is more blurry than that obtained by the proposed model. Thus, we demonstrate that our model achieves a transformed image with clearer texture than the fluid approach.

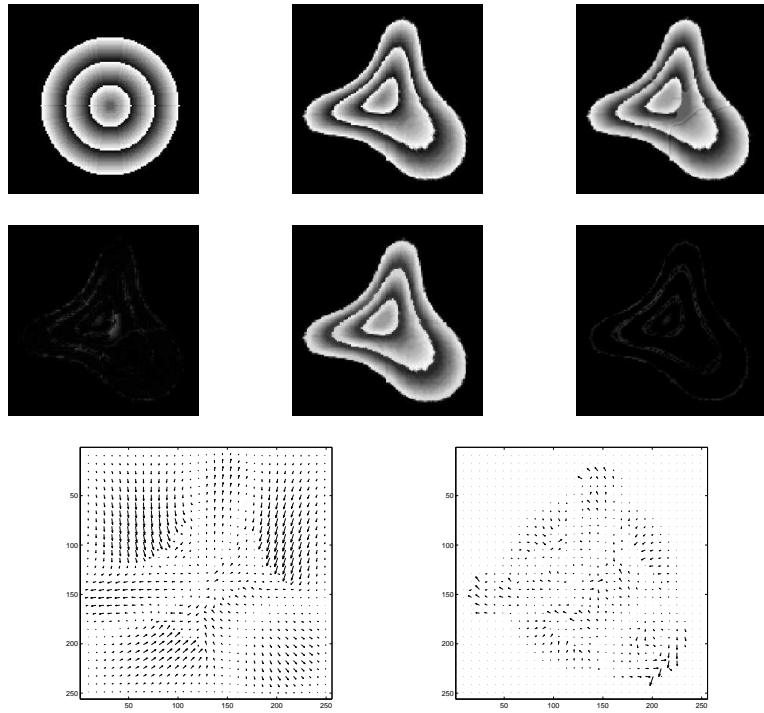


Figure 2: qualitative results of experiment 2. From left to right, top to bottom: (a)template image; (b)target image; (c)transformed image obtained by fluid model; (d)difference image between (b) and (c); (e)transformed image obtained by proposed model; (f)difference image between (b) and (e); (g)displacement map obtained by fluid model; (h)displacement map obtained by proposed model.

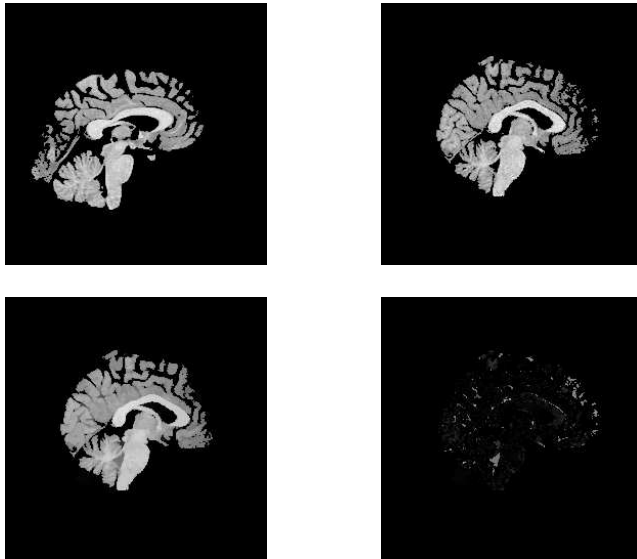


Figure 3: qualitative results of experiment 3. From left to right, top to bottom: (a)template image; (b)target image; (c)transformed image obtained by fluid model; (d)difference image between (b) and (c); (e)transformed image obtained by proposed model; (f)difference image between (b) and (f).

The third experiment is designed to demonstrate that our model can capture complex deformations in medical images. The test data is an MRI image of human brain with size  $256 \times 256$  pixels. The results are shown in Figure 3. The registration has successfully transformed the template image towards the target image, and the transformed image persists sharp edges.

To further assess the quality of the registration in the above experiments, mean and variance of the squared sum of intensity difference (SSD), and correlation coefficient (CC) have been calculated and are listed in tables 2.

## 5 CONCLUSIONS

In this paper we present a novel registration technique expressed in a particle framework. It is an inviscid model designed for nonrigid registration problems. The key features of our model are (a) it can accommodate both small and large deformations, (b) it overcomes the blurring drawback of fluid models and achieves transformed images with clear textures and sharp edges, (c) it is very simple and fast. We have demonstrated the performance of our approach on a variety of images including synthetic and real data. The results of experiments are desiring and satisfying. Future efforts will be made to explore more complicated simulation frameworks where internal interaction is added to particle systems.

Experiment 1	Mean(SSD)	Var(SSD)	CC
No registration	0.103760	0.092994	0.447277
Fluid	0.000271	0.000027	0.998853
Proposed	0.000017	0.000000	0.999968
Experiment 2	Mean(SSD)	Var(SSD)	CC
No registration	0.137189	0.056491	0.385506
Fluid	0.000899	0.000023	0.995851
Proposed	0.000738	0.000014	0.996772
Experiment 3	Mean(SSD)	Var(SSD)	CC
No registration	0.054380	0.021933	0.523169
Fluid	0.002417	0.000278	0.977904
Proposed	0.001993	0.000439	0.981655

Table 2: qualitative measure for 3 experiments

## References

- [1] R. Bajcsy and S. Kovacic. Multiresolution elastic matching. *Computer Vision, Graphics, and Image Processing*, 46:1–21, 1989.
- [2] M. Bro-Nielsen and C. Gramkow. Fast fluid registration of medical images. In *Proc. Visualization in Biomedical Computing*, pages 267–276, 1996.
- [3] C. Broit. *Optimal registration of deformed images*. PhD thesis, University of Pennsylvania, 1981.
- [4] G.E. Christensen, S.C. Joshi, and M.I. Miller. Volumetric transformation of brain anatomy. *IEEE Trans. Medical Imaging*, 16:864–877, 1997.
- [5] G.E. Christensen, R.D. Rabbitt, and M.I. Miller. A deformable neuroanatomy textbook based on viscous fluid mechanics. In *Proc. Information Science and Systems*, pages 211–216, 1993.
- [6] G.E. Christensen, R.D. Rabbitt, and M.I. Miller. Deformable templates using large deformation kinematics. *IEEE Trans. Image Processing*, 5:1435–1447, 1996.
- [7] S. Clavet, P. Beaudoin, and P. Poulin. Particle-based viscoelastic fluid simulation. *Eurographics/ACM SIGGRAPH Symp. Computer Animation*, 2005. To appear.
- [8] C. Davatzikos. Spatial transformation and registration of brain images using elastically deformable models. *Computer Vision and Image Understanding*, 66:207–222, 1997.
- [9] L.D. Landau and E.M. Lifshitz. *Fluid Mechanics*. Pergamon, 1987.

- [10] D. Ruechert. Nonrigid registration: techniques and applications. *Medical Image Registration*, 13:281–302, 2001.
- [11] B.C. Vemuri, J. Ye, Y. Chen, and C.M. Leonard. Image registration via level-set motion: applications to atlas-based segmentation. *IEEE Trans. Medical Image Analysis*, 7:1–20, 2003.
- [12] G. Wollny and F. Kruggel. Computational cost of nonrigid registration algorithms based on fluid dynamics. *IEEE Trans. Medical Imaging*, 21:946–952, 2002.